



Observing Application

Date : Feb, 01 2010
Proposal ID : VLA/10B-153
Legacy ID : AB1358
PI : Shea Brown
Type : Regular
Category : Extragalactic
Total Time : 48.9

EVLA Deep Cluster Survey: Pilot Study

Abstract:

The overall goal of this project is to use the relativistic plasma in and around clusters of galaxies to probe the dynamics of cluster baryons during a critical epoch of large-scale structure formation. We propose moderately deep, 1.4~GHz polarized continuum observations of 30 high-redshift ($z=0.35-0.9$) clusters of galaxies from the Chandra Cluster Cosmology Project. The primary goals of this pilot survey are: 1) Characterize the Mpc-scale radio halo population in an unexplored redshift and X-ray luminosity regime, verifying theoretically important scaling relations down to lower cluster masses; 2) Directly test turbulent re-acceleration models of giant radio halos through independent confirmation of the bi-modal nature of the population; 3) Conduct a deep polarization search for external shocks in the outer infall regions of the clusters. These high-mach shocks pre-accelerate cosmic-ray electrons and feed clusters long-lived and thermodynamically important CR protons; 4) Identify the most critical questions for the design of an EVLA Deep Cluster Survey to probe CR physics and the dynamic evolution of cluster baryons over cosmic time; 5) Identify interesting or extreme systems for multiwavelength study beyond the future deep survey parameters.

Authors:

Name	Institution	Email	Status
Shea Brown	Australia Telescope National Facility	brown@physics.umn.edu	
Nicholas Battaglia	Toronto, University of	battaglia@astro.utoronto.ca	Graduating: Thesis: false
Jean Eilek	National Radio Astronomy Observatory	jeilek@aoc.nrao.edu	
Thomas Jones	Minnesota, University of	twj@astro.umn.edu	
Rupal Mittal	Rochester Institute of Technology	rmittal@astro.rit.edu	
Frazer Owen	National Radio Astronomy Observatory	fowen@nrao.edu	
Christoph Pfrommer	Toronto, University of	pfrommer@cita.utoronto.ca	
Thomas Reiprich	Universitat Bonn	reiprich@astro.uni-bonn.de	
Ken Rines	Western Washington University	Ken.Rines@wwu.edu	
Lawrence Rudnick	Minnesota, University of	larry@astro.umn.edu	
Alexey Vikhlinin	Harvard-Smithsonian Center for Astrophysics	alexey@head.cfa.harvard.edu	

Principal Investigator: Shea Brown
Contact: Shea Brown
Telephone: +61 2 9372 4380
Email: brown@physics.umn.edu

Related proposals:

Joint:

Not a Joint Proposal

Observing type(s):

Continuum, Polarimetry

VLA Resources

Name	Conf.	Frontend & Backend	Setup
B-array	B	L Band 20 cm 1000 - 2000 MHz WIDAR OSRO1: 2 Subbands/Full polz	Rest frequencies: 1350.0, 1664.0 MHz Bandwidth: 128.0 MHz No. of Channels: 64 Poln. products: 4.0 Channel Width: 2000.0 kHz
C-array	C	L Band 20 cm 1000 - 2000 MHz WIDAR OSRO1: 2 Subbands/Full polz	Rest frequencies: 1350.0, 1664.0 MHz Bandwidth: 128.0 MHz No. of Channels: 64 Poln. products: 4.0 Channel Width: 2000.0 kHz
BnA-array	BnA	L Band 20 cm 1000 - 2000 MHz WIDAR OSRO1: 2 Subbands/Full polz	Rest frequencies: 1350.0, 1664.0 MHz Bandwidth: 128.0 MHz No. of Channels: 64 Poln. products: 4.0 Channel Width: 2000.0 kHz
CnB-array	CnB	L Band 20 cm 1000 - 2000 MHz WIDAR OSRO1: 2 Subbands/Full polz	Rest frequencies: 1350.0, 1664.0 MHz Bandwidth: 128.0 MHz No. of Channels: 64 Poln. products: 4.0 Channel Width: 2000.0 kHz

Sources:

Name	Position		Velocity		Group
CIGJ0159+0030	Coordinate System	Equatorial	Convention	Radio	LST 0
	Equinox	J2000			
	Right Ascension	01:59:18.19 00:00:00.0	Ref. Frame	LSRK	
	Declination	+00:30:11 00:00:00	Redshift	0.386	
CIGJ0926+1242	Coordinate System	Equatorial	Convention	Radio	LST 0
	Equinox	J2000			
	Right Ascension	09:26:36.6 00:00:00.0	Ref. Frame	LSRK	
	Declination	+12:42:56 00:00:00	Redshift	0.489	
CIGJ0230+1836	Coordinate System	Equatorial	Convention	Radio	LST 0
	Equinox	J2000			
	Right Ascension	02:30:26.59 00:00:00.0	Ref. Frame	LSRK	
	Declination	+18:36:21 00:00:00	Velocity	0.799	

Name	Position		Velocity		Group
CIGJ0030+2618	Coordinate System	Equatorial	Convention	Radio	LST 0
	Equinox	J2000			
	Right Ascension	00:30:33.19 00:00:00.0	Ref. Frame	LSRK	
	Declination	+26:18:19 00:00:00	Redshift	0.500	
CIGJ0809+2811	Coordinate System	Equatorial	Convention	Radio	LST 0
	Equinox	J2000			
	Right Ascension	08:09:40.99 00:00:00.0	Ref. Frame	LSRK	
	Declination	+28:11:57 00:00:00	Velocity	0.399	
CIGJ0956+4107	Coordinate System	Equatorial	Convention	Radio	LST 0
	Equinox	J2000			
	Right Ascension	09:56:03.4 00:00:00.0	Ref. Frame	LSRK	
	Declination	+41:07:14 00:00:00	Redshift	0.587	
CIGJ0958+4702	Coordinate System	Equatorial	Convention	Radio	LST 0
	Equinox	J2000			
	Right Ascension	09:58:19.39 00:00:00.0	Ref. Frame	LSRK	
	Declination	+47:02:11 00:00:00	Velocity	0.39	
CIGJ0853+5759	Coordinate System	Equatorial	Convention	Radio	LST 0
	Equinox	J2000			
	Right Ascension	08:53:14.1 00:00:00.0	Ref. Frame	LSRK	
	Declination	+57:59:39 00:00:00	Redshift	0.475	
CIGJ0318-0302	Coordinate System	Equatorial	Convention	Radio	LST 0
	Equinox	J2000			
	Right Ascension	03:18:17.29 00:00:00.0	Ref. Frame	LSRK	
	Declination	-3:01:20 00:00:00	Redshift	0.37	
CIGJ0302-0423	Coordinate System	Equatorial	Convention	Radio	LST 0
	Equinox	J2000			
	Right Ascension	03:02:21.29 00:00:00.0	Ref. Frame	LSRK	
	Declination	-4:23:29 00:00:00	Velocity	0.3501	
CIGJ0152-1358	Coordinate System	Equatorial	Convention	Radio	LST 0
	Equinox	J2000			
	Right Ascension	01:52:40.99 00:00:00.0	Ref. Frame	LSRK	
	Declination	-13:57:45 00:00:00	Redshift	0.8325	
CIGJ1701+6414	Coordinate System	Equatorial	Convention	Radio	LST 12
	Equinox	J2000			
	Right Ascension	17:01:30.22 00:00:00.0	Ref. Frame	LSRK	
	Declination	+64:12:05 00:00:00	Redshift	0.4530	
CIGJ1524+0957	Coordinate System	Equatorial	Convention	Radio	LST 12
	Equinox	J2000			
	Right Ascension	15:24:40.3 00:00:00.0	Ref. Frame	LSRK	
	Declination	+09:57:38 00:00:00	Redshift	0.5160	

Name	Position		Velocity		Group
CIGJ1120+2326	Coordinate System	Equatorial	Convention	Radio	LST 12
	Equinox	J2000			
	Right Ascension	11:20:57.9 00:00:00.0	Ref. Frame	LSRK	
	Declination	+23:26:40	Redshift	0.562	
		00:00:00			
CIGJ1212+2733	Coordinate System	Equatorial	Convention	Radio	LST 12
	Equinox	J2000			
	Right Ascension	12:12:19.2 00:00:00.0	Ref. Frame	LSRK	
	Declination	+27:33:14	Velocity	0.3533	
		00:00:00			
CIGJ1222+2709	Coordinate System	Equatorial	Convention	Radio	LST 12
	Equinox	J2000			
	Right Ascension	12:22:01.9 00:00:00.0	Ref. Frame	LSRK	
	Declination	+27:09:19	Velocity	0.472	
		00:00:00			
CIGJ1003+3253	Coordinate System	Equatorial	Convention	Radio	LST 12
	Equinox	J2000			
	Right Ascension	10:03:04.9 00:00:00.0	Ref. Frame	LSRK	
	Declination	+32:54:28	Redshift	0.4161	
		00:00:00			
CIGJ1226+3332	Coordinate System	Equatorial	Convention	Radio	LST 12
	Equinox	J2000			
	Right Ascension	12:26:58.9 00:00:00.0	Ref. Frame	LSRK	
	Declination	+33:32:47	Redshift	0.8877	
		00:00:00			
CIGJ1312+3900	Coordinate System	Equatorial	Convention	Radio	LST 12
	Equinox	J2000			
	Right Ascension	13:12:19.39 00:00:00.0	Ref. Frame	LSRK	
	Declination	+39:00:57	Velocity	0.4037	
		00:00:00			
CIGJ1641+4001	Coordinate System	Equatorial	Convention	Radio	LST 12
	Equinox	J2000			
	Right Ascension	16:41:52.5 00:00:00.0	Ref. Frame	LSRK	
	Declination	+40:01:28	Redshift	0.464	
		00:00:00			
CIGJ1120+4318	Coordinate System	Equatorial	Convention	Radio	LST 12
	Equinox	J2000			
	Right Ascension	11:20:07.5 00:00:00.0	Ref. Frame	LSRK	
	Declination	+43:18:05	Velocity	0.600	
		00:00:00			
CIGJ1416+4446	Coordinate System	Equatorial	Convention	Radio	LST 12
	Equinox	J2000			
	Right Ascension	14:16:28.69 00:00:00.0	Ref. Frame	LSRK	
	Declination	+44:46:41	Redshift	0.400	
		00:00:00			
CIGJ1221+4918	Coordinate System	Equatorial	Convention	Radio	LST 12
	Equinox	J2000			
	Right Ascension	12:21:24.49 00:00:00.0	Ref. Frame	LSRK	
	Declination	+49:18:12	Redshift	0.700	
		00:00:00			

Name	Position		Velocity		Group
CIGJ1334+5030	Coordinate System	Equatorial	Convention	Radio	LST 12
	Equinox	J2000			
	Right Ascension	13:34:19.99	Ref. Frame	LSRK	
		00:00:00.0			
	Declination	+50:30:54 00:00:00	Redshift	0.620	
CIGJ1202+5751	Coordinate System	Equatorial	Convention	Radio	LST 12
	Equinox	J2000			
	Right Ascension	12:02:13.69	Ref. Frame	LSRK	
		00:00:00.0			
	Declination	+57:51:52 00:00:00	Velocity	0.6775	
CIGJ1002+6858	Coordinate System	Equatorial	Convention	Radio	LST 12
	Equinox	J2000			
	Right Ascension	10:02:07.69	Ref. Frame	LSRK	
		00:00:00.0			
	Declination	+68:58:48 00:00:00	Velocity	0.5	
CIGJ1354-0221	Coordinate System	Equatorial	Convention	Radio	LST 12
	Equinox	J2000			
	Right Ascension	13:54:16.9	Ref. Frame	LSRK	
		00:00:00.0			
	Declination	-2:21:47 00:00:00	Redshift	0.546	
CIGJ1357+6232	Coordinate System	Equatorial	Convention	Radio	LST 12
	Equinox	J2000			
	Right Ascension	13:57:19.39	Ref. Frame	LSRK	
		00:00:00.0			
	Declination	+62:32:42 00:00:00	Velocity	0.525	
CIGJ0333-2456	Coordinate System	Equatorial	Convention	Radio	LST 0 Low-Dec
	Equinox	J2000			
	Right Ascension	03:33:10.19	Ref. Frame	LSRK	
		00:00:00.0			
	Declination	-24:56:40 00:00:00	Velocity	0.4751	
CIGJ0328-2140	Coordinate System	Equatorial	Convention	Radio	LST 0 Low-Dec
	Equinox	J2000			
	Right Ascension	03:28:36.1	Ref. Frame	LSRK	
		00:00:00.0			
	Declination	-21:40:04 00:00:00	Velocity	0.5901	

Sessions:

Name	Session Time (hours)	Repeat	Separation	LST minimum	LST maximum	Elevation Minimum
0 LST C-array	0.90	11	0 day	00:00:00	24:00:00	0
0 LST CnB-array	0.90	2	0 day	00:00:00	24:00:00	0
0 LST B-array	0.73	11	0 day	00:00:00	24:00:00	0
0 LST BnA-array	0.73	2	0 day	00:00:00	24:00:00	0
12 LST C-array	0.90	17	0 day	00:00:00	24:00:00	0
12 LST B-array	0.73	17	0 day	00:00:00	24:00:00	0

Session Constraints:

Name	Constraints	Comments

Session Source/Resource Pairs:

Session Name	Source	Resource	Time	Figure of Merit	Subarray
0 LST C-array	CIGJ0159+0030 CIGJ0926+1242 CIGJ0230+1836 CIGJ0030+2618 CIGJ0809+2811 CIGJ0956+4107 CIGJ0958+4702 CIGJ0853+5759 CIGJ0318-0302 CIGJ0302-0423 CIGJ0152-1358	C-array	0.9 hour	21 mJy/bm	
0 LST CnB-array	CIGJ0333-2456 CIGJ0328-2140	CnB-array	0.9 hour	21 mJy/bm	
0 LST B-array	CIGJ0159+0030 CIGJ0926+1242 CIGJ0230+1836 CIGJ0030+2618 CIGJ0809+2811 CIGJ0956+4107 CIGJ0958+4702 CIGJ0853+5759 CIGJ0318-0302 CIGJ0302-0423 CIGJ0152-1358	B-array	0.73 hour	21 mJy/bm	
0 LST BnA-array	CIGJ0333-2456 CIGJ0328-2140	BnA-array	0.73 hour	21 mJy/bm	
12 LST C-array	CIGJ1701+6414 CIGJ1524+0957 CIGJ1120+2326 CIGJ1212+2733 CIGJ1222+2709 CIGJ1003+3253 CIGJ1226+3332 CIGJ1312+3900 CIGJ1641+4001 CIGJ1120+4318 CIGJ1416+4446 CIGJ1221+4918 CIGJ1334+5030 CIGJ1202+5751 CIGJ1002+6858 CIGJ1354-0221 CIGJ1357+6232	C-array	0.9 hour	21 mJy/bm	

Session Name	Source	Resource	Time	Figure of Merit	Subarray
12 LST B-array	CIGJ1701+6414 CIGJ1524+0957 CIGJ1120+2326 CIGJ1212+2733 CIGJ1222+2709 CIGJ1003+3253 CIGJ1226+3332 CIGJ1312+3900 CIGJ1641+4001 CIGJ1120+4318 CIGJ1416+4446 CIGJ1221+4918 CIGJ1334+5030 CIGJ1202+5751 CIGJ1002+6858 CIGJ1354-0221 CIGJ1357+6232	B-array	0.73 hour	21 mJy/bm	

Present for observation: no

Staff support: Consultation

Plan of Dissertation: no

EVLA Deep Cluster Survey: Pilot

Synchrotron Probes of High-Redshift Cluster Mergers

Summary

The overall goal of this project is to use the relativistic plasma in and around clusters of galaxies to probe the dynamics of cluster baryons during a critical epoch of large-scale structure formation. We propose moderately deep, full Stokes, 1.4 GHz continuum observations of 30 high-redshift ($z = 0.35 - 0.9$) clusters of galaxies from the *Chandra Cluster Cosmology Project* (CCCP: Vikhlinin et al. 2008). The C-configuration observations proposed here have the critical combination of resolution and surface-brightness sensitivity to probe for large-scale synchrotron features at these redshifts, while the B configuration observations are critical to remove the cluster radio galaxies. The primary goals of this pilot survey are: 1) Characterize the Mpc-scale radio halo population in an unexplored redshift and X-ray luminosity regime, verifying theoretically important scaling relations down to lower cluster masses; 2) Directly test turbulent re-acceleration models of giant radio halos (GRH) through independent confirmation of the bi-modal nature of the population (Brunetti et al. 2009; Venturi et al. 2007); 3) Conduct a deep polarization search for external shocks in the outer infall regions of the clusters. These high-mach shocks pre-accelerate cosmic-ray electrons (CRe) and feed clusters long-lived and thermodynamically important CR protons; 4) Identify the most critical questions for the design of an *EVLA Deep Cluster Survey* to probe CR physics and the dynamic evolution of cluster baryons over cosmic time; 5) Identify interesting systems (particularly bright or extended, polarized structure) for deep study beyond the future well-defined survey parameters.

These observations, when combined with the CCCP *Chandra* data and subsequent aggressive optical/infrared follow-up, will explore the diagnostic power of radio for non-thermal/non-equilibrium processes in clusters. This is of enormous interest to cluster cosmology studies; an important task of these observations will be to determine to what extent the radio band can aid in these efforts, in preparation for an *EVLA DCS*.

Science Justification

Current radio observations reveal spectacular Mpc-scale synchrotron emission associated with some massive clusters of galaxies, while other clusters of comparable mass show no sign of diffuse radio emission even at much lower luminosity limits. The origins of the cosmic-ray (CR) leptons and large-scale μG magnetic fields themselves are still an open question, though a clear correlation with merging or dynamically accreting clusters has emerged (e.g., Brunetti et al. 2009). This emission is an indicator of recent energy input into the intra-cluster medium (ICM), whether through merger/accretion shocks or AGN outflows, and its properties can be used to trace dynamical activity in low-density regions inaccessible at other wavelengths (e.g., Rudnick et al. 2009). However, interpretation of the synchrotron emission is model dependent, and relies heavily on an understanding of the *origin* of the CR electrons and magnetic fields. There are a variety of models for the acceleration and propagation of CR protons and electrons in large-scale structure; most predict a sea of low surface-brightness synchrotron emission permeating the cosmic-web, the peaks of which are in massive clusters of galaxies which we observe as GRHs. There are two broad potential sources for the cosmic-ray electrons (CRe) in the ICM; electrons directly accelerated by accretion/merger shocks and/or cluster turbulence (primary models), and electrons created from relativistic proton-proton collisions from cosmic-ray protons (CRp) that are accelerated during large-scale structure formation and trapped via magnetic fields in clusters for a Hubble time (secondary models, e.g., Basi et al 2007). There are variations in both models based on the details of where and how the CR are accelerated, though none of the models

explain the recent observational data. Recent efforts to construct a “unified model” for GRHs and radio relics (Pfrommer et al. 2008) using both primary and secondary models represent the next step in complexity, though observational constraints are needed to limit the available parameter space.

This shortfall in our understanding is made even more poignant because the non-thermal energy/pressure and large-scale magnetic field have substantial influences on the thermal properties of the ICM (Maron et al. 2004), and indicate deviations from hydrostatic equilibrium which is a critical assumption for cosmological analysis. Diffuse radio emission in clusters of galaxies currently provide our *only* window into this relativistic particle population, although there are attempts with *Fermi* to observe the γ -rays from CRp collisions.

Pilot Observations: Filling in the L_R vs. L_X Plane

Recent observational attempts to use a large sample of clusters to constrain CR acceleration models and their relation to cluster dynamics have begun to yield results (e.g., Venturi et al. 2007, Donnert et al. 2009). Brunetti et al. (2009) used the *GMRT Radio Halo Survey (RHS)* ($z = 0.2 - 0.4$ clusters), along with observation taken from the literature, to show that X-ray clusters are bi-modal in their diffuse radio properties. They find that only $\sim 1/3$ of clusters host large-scale diffuse emission (with the radio luminosity correlated with the X-ray luminosity), while the rest are radio quiet (Fig. 1). This favors a turbulent re-acceleration model for the origin of radio halos, since the post-merger CRe have only ~ 100 Myr radiative lifetimes, though given the complexity of cluster physics, secondary models cannot be ruled out (e.g., Kushnir, Katz & Waxman 2009).

For an initial pilot, we propose moderately deep ($21 \mu\text{Jy beam}^{-1}$, see below) 1.4 GHz C-configuration observations of the entire high-redshift sample of the *Chandra Cluster Cosmology Project* (Vikhlinin et al. 2008). The $\sim 15''$ resolution of the C-array (see Figure 2) is ideal for detecting halo emission at redshifts > 0.3 (e.g., Bonafede et al. 2009), and the polarization observations will allow for the identification of shock-structures such as peripheral relics. However, these structures on scales of 250-1000 kpc must be distinguished from smaller, and possibly multiple radio galaxies, so B configuration are critical. The *CCCP* cluster sample will extend the *GMRT RHS* results into lower X-ray luminosity ($0.68 - .42 \times 10^{44} \text{ erg s}^{-1}$) and mass ($1.0 - 9.9 \times 10^{14} M_\odot$) regime, which will verify to what extent the scaling relations, used as the underpinning of theoretical investigations of ICM physics (Figure 1), hold at lower mass (X-ray luminosity).

The issue of “contamination” from radio galaxies to the halo’s total flux is important at these redshifts. For the immediate science goals of this pilot, we will need to separate extended radio galaxies from other sources of CRe (e.g., shocks and smooth turbulence driven halo emission). Therefore, we propose for a similarly shallow B-configuration ($5''$), full Stokes survey of the *CCCP* sample in order to appropriately deal with this issue. Figure 2 illustrates the angular scales involved. The *Chandra* color image is of cl1524+0927 ($z=0.5$) with FIRST ($5''$; green contours), NVSS ($45''$; white contours) and $15''$ C-array beam (white circle) overlaid. Over the $z=0.35-0.9$ redshift range of the *CCCP* sample,

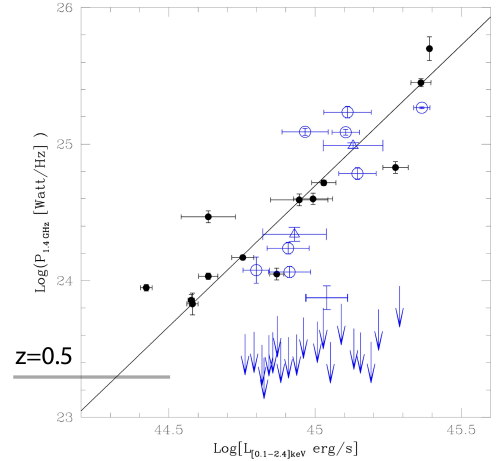


Figure 1: Plot from Brunetti et al. (2009) showing cluster radio halo luminosity vs. X-ray luminosity. The open circles and upper limits are from the GMRT Radio Halo Survey. The grey line shows the 3σ detection threshold for the current proposal for a $z=0.5$ cluster, extending over the X-ray luminosity range of the *CCCP* sample.

5'' (15'') is 25-39 kpc (74-117 kpc).

EVLA Deep Cluster Survey

In addition to the important science output described above, these observations serve as a pilot study for a much larger *EVLA Deep Cluster Survey* using the CCCP cluster sample. The *EVLA DCS* will be a deep, multi-resolution polarization survey (D, C, and B configurations, supplemented by A at the highest redshifts) over the entire 1-2 GHz range of the EVLA L-band, allowing high quality imaging of the halo structures.

The combination of deep polarization and multi-scale imaging is critical for disentangling the various sources of CRe, which in turn is necessary for relating synchrotron emission to the dynamics of the baryonic ICM. The *EVLA DCS* will also provide a versatile legacy data-set that can be used to address outstanding questions regarding the dynamics and evolution of the ICM. We outline a sample of these questions below, along with why and larger *EVLA DCS* is necessary to achieve these goals:

CLUSTER THERMODYNAMICS: When and how does the ICM become energized, e.g., through merger/accretion shocks, AGN, SNe? The answer will certainly depend on cluster mass and redshift; on the galaxy group scale, non-gravitational feedback processes will have a larger impact. *Need a factor of ~ 10 improvement in polarized surface-brightness sensitivity in B and A-arrays to detect thermalizing internal shocks;*

CLUSTER COSMOLOGY: What are the implications of the type of energy injection on the cluster profiles (density/temperature/pressure/entropy)? This helps to understand the properties and formation of SZ/X-ray profiles and their redshift-evolution (where we have poorer data from SZ and X-rays). Answering this question will be crucial in inferring cosmological parameters from SZ/X-ray number counts, SZ power spectrum, and gas-fraction. Radio is completely *complementary* to these traditional probes. In particular, the *primary* radio emission serves as a snapshot of current structure formation, while the *secondary* hadronic one gives a time-integrated census of the non-thermal activity. *Need as above for the internal shocks (primary emission), and $2\text{-}3\times$ the sensitivity over all the arrays to separate radio galaxies from the core hadronic component;*

ELECTRON SHOCK-ACCELERATION: What are the dominant acceleration processes? Recent work (e.g. Markevitch et al. 2005: Abell 520) shows that even weak shocks ($M < \sim 2$) can accelerate electrons. This is completely unexpected from the study of solar system and SNR shocks. *Need as above for internal shocks;*

CLUSTER ARCHEOLOGY: Radio information can help disentangle the history of individual clusters by taking into account the different cooling times of the underlying electron populations (primary, secondary, re-accelerated). Characterizing the AGN components of the radiation will be crucial in calibrating cosmological simulations with AGN feedback. *The pilot observations will trace cluster AGN activity over the CCCP sample (e.g., Mittal et al. 2009), but we need the above improvements in sensitivity for separating different sources of CRe.*

With the completeness and quality of the CCCP sample, we will be able to explore these properties as functions of cluster X-ray luminosity, redshift and dynamical state. The pilot study proposed here, in addition to its direct scientific contributions, will provide important input on such issues as optimum resolution, halo vs. AGN contrasts, polarization sensitivity, etc. for the design of the full survey.

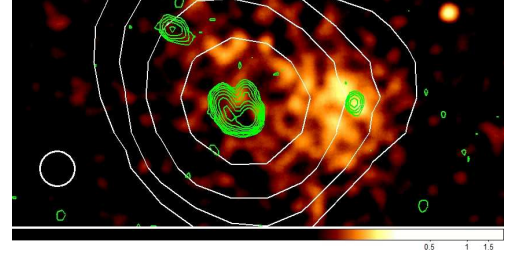


Figure 2: Color: *Chandra* image of the $z=0.5$ cluster CL1524+0957; Green: FIRST image showing a narrow-angle tailed (NAT) radio galaxy whose jets are bent by ICM pressure; White: NVSS; White Circle: C-array beam.

Source Selection

The *Chandra Cluster Cosmology Project* (Vikhlinin et al. 2008), is a complete high-redshift sub-sample of the 400d survey (Burenin et al. 2007). The CCCP consists of 36 clusters at $z = 0.35 - 0.9$ with $\langle z \rangle \sim 0.5$ and 49 low-redshift clusters with $z = 0.025 - 0.2$, all followed-up with moderately deep *Chandra* observations. Extensive optical and infrared follow-up projects on the CCCP sample include MMT weak lensing measurements (Israel et al. 2009) and *Spitzer* analysis of cluster star-formation (e.g., Rines et al. 2007).

We are limiting the *EVLA DCS* pilot study to only the high-redshift sample with $\delta > -30$, which totals 30 clusters. These observations will not provide the detailed structures of halos that can be done at low redshifts. However, this sample will be extremely valuable as a legacy data set because: 1) We are systematically exploring a *new* redshift, luminosity, mass regime; 2) We can be sure that typical GRH emission will be well within the primary beam, while also sampling the critical infall and super-cluster outer regions; 3) Clusters at redshifts > 0.5 show increased fraction of mergers; 22 of the 30 clusters in our sample are designated as merging by Vikhlinin et al. (2008);

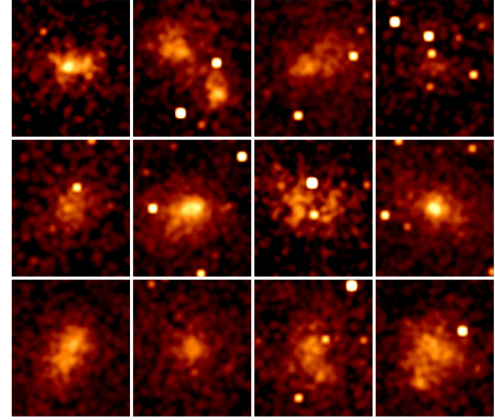


Figure 3: X-ray emission from the 12 of the highest redshift clusters ($z > 0.5$) in the CCCP sample from Vikhlinin et al. (2008), which show a statically significant lower fraction of cooling-cores and higher fraction of merger activity.

Technical Requirements

To meet the primary science goals we must achieve a detection threshold of $\sim 2 \times 10^{23}$ Watt Hz^{-1} at 1.4 GHz. It is sufficient to reach a $\sigma_{rms} = 21 \mu\text{Jy beam}^{-1}$ (or ~ 33.2 mK) in C-configuration with 2×128 MHz bands in the 1-2 GHz range (calculated assuming a centrally peaked halo with a 2.5σ core of diameter 0.25 Mpc and ΛCDM cosmology),

to reach this threshold for a $z=0.5$ cluster, which is where the bulk of our source lay (18 out of 30 have $0.4 < z < 0.6$). We should note that simplified detection threshold calculations (like we present here) tend to overestimate the threshold compared to those calculated with simulated halo emission (e.g., Venturi et al. 2007). This will take (0.7 source + 0.2 overhead) hours per cluster, for a total of 27 hours. For the B-configuration data, we would like to also reach $\sigma_{rms} = 21 \mu\text{Jy beam}^{-1}$, which will take (0.53 source + 0.2 overhead) hours per cluster, for a total of 21.9 hours. We therefore request a total of 48.9 hours spread out over C, CnB, B, and BnA configurations.

References

- Battaglia, N., Pfrommer, C., Sievers, J. L., Bond, J. R., & Enßlin, T. A. 2009, MNRAS, 393, 1073
 Brown, S., & Rudnick, L. 2009, AJ, 137, 3158
 Brunetti, G., Cassano, R., Dolag, K., & Setti, G. 2009, A&A, 507, 661
 Burenin, R. A., Vikhlinin, A., Hornstrup, A., Ebeling, H., Quintana, H., & Mescheryakov, A. 2007, ApJS, 172, 561
 Donnert, J., Dolag, K., Brunetti, G., Cassano, R., & Bonafede, A. 2009, MNRAS, 1630
 Israel, H., et al. 2009, arXiv:0911.3111
 Kushnir, D., Katz, B., & Waxman, E. 2009, Journal of Cosmology and Astro-Particle Physics, 9, 24
 Markevitch, M., Govoni, F., Brunetti, G., & Jerius, D. 2005, ApJ, 627, 733
 Mittal, R., Hudson, D. S., Reiprich, T. H., & Clarke, T. 2009, A&A, 501, 835
 Pfrommer, C., Enßlin, T. A., & Springel, V. 2008, MNRAS, 385, 1211
 Rines, K., Finn, R., & Vikhlinin, A. 2007, ApJ, 665, L9
 Venturi, T., Giacintucci, S., Brunetti, G., Cassano, R., Bardelli, S., Dallacasa, D., & Setti, G. 2007, A&A, 463, 937
 Vikhlinin, A., et al. 2009, ApJ, 692, 1033